Paraneoplastic Antigen-Like 5 Gene (*PNMA5*) Is Preferentially Expressed in the Association Areas in a Primate Specific Manner

Masafumi Takaji[1,2], Yusuke Komatsu[1], Akiya Watakabe[1,2], Tsutomu Hashikawa[3] and Tetsuo Yamamori[1,2,4]

[1]Division of Brain Biology, National Institute for Basic Biology, 38 Nishigonaka Myodaiji, Okazaki 444-8585, Japan, [2]Department of Basic Biology, The Graduate University for Advanced Studies, 38 Nishigonaka Myodaiji, Okazaki 444-8585, Japan, [3]Laboratory for Neural Architecture, Brain Science Institute, RIKEN, Wako 351-0198, Japan and [4]National Institute for Physiological Sciences, 38 Nishigonaka Myodaiji, Okazaki 444-8585, Japan

M.T. and Y.K. contributed equally to this paper

To understand the relationship between the structure and function of primate neocortical areas at a molecular level, we have been screening for genes differentially expressed across macaque neocortical areas by restriction landmark cDNA scanning (RLCS). Here, we report enriched expression of the paraneoplastic antigen-like 5 gene (*PNMA5*) in association areas but not in primary sensory areas, with the lowest expression level in primary visual cortex. In situ hybridization in the primary sensory areas revealed *PNMA5* mRNA expression restricted to layer II. Along the ventral visual pathway, the expression gradually increased in the excitatory neurons from the primary to higher visual areas. This differential expression pattern was very similar to that of retinol-binding protein (RBP) mRNA, another association-area-enriched gene that we reported previously. Additional expression analysis for comparison of other genes in the *PNMA* gene family, *PNMA1*, *PNMA2*, *PNMA3*, and *MOAP1* (*PNMA4*), showed that they were widely expressed across areas and layers but without the differentiated pattern of *PNMA5*. In mouse brains, *PNMA1* was only faintly expressed and *PNMA5* was not detected. Sequence analysis showed divergence of *PNMA5* sequences among mammals. These findings suggest that *PNMA5* acquired a certain specialized role in the association areas of the neocortex during primate evolution.

Keywords: association area evolution, cortical structure, in situ hybridization, neocortex, primate specific

The neocortex has undergone a marked increase in volume and complexity during the course of primate evolution (Stephan et al. 1981; Haug, 1987; Preuss and Goldman-Rakic 1991c; Finlay and Darlington 1995). Brodmann, who conducted comprehensive surveys of the mammalian cytoarchitecture, concluded that the granular frontal cortex is rudimentary or absent in mammals other than primates, but in primates it underwent considerable expansion with the concomitant addition of new areas during evolution (Brodmann 1909, 1912). Consistent with this classic study, Preuss and Goldman-Rakic also suggested that anthropoid primates evolved additional cortical areas during their phylogenetic history (Preuss and Goldman-Rakic 1991a, 1991b, 1991c). This idea was based on the more elaborate cytoarchitectonic and connectional subdivisions in the frontal, parietal and temporal areas in *Macaca* as compared with *Galago*, particularly in the granular frontal and superior temporal polysensory cortices. The new areas that emerged during primate evolution correspond to higher-order association areas, the regions that receive inputs from sensory and other association areas (Pandya and Kuypers 1969; Jones and Powell 1970; Mesulam et al. 1977; Pandya and Seltzer 1982), and which mediate integrative aspects of somatosensory and visuospatial (Friedman et al. 1986; Andersen 1989), auditory (Leinonen et al. 1980; Galaburda and Pandya 1983), polysensory (Bruce et al. 1981; Baylis et al. 1987), and memory processes (Van Hoesen 1982). These structures influence perception, cognition, or behavior in part through their strong connections with the frontal lobe (Bignall and Imbert 1969; Milner and Petrides 1984; Goldman-Rakic 1988; Pandya and Yeterian 1990). Because of such divergence of functions, it still remains a challenge to answer "what is the nature of association areas?". To solve this problem, applying molecular genetic approaches is potentially very effective (Crick 1999).

Previous studies have demonstrated the heterogeneous distribution of various neurochemicals and neurotransmitter receptors within the adult primate neocortex (Mash et al. 1988; Bloom et al. 1997; Pimenta et al. 2001; Zilles et al. 2002). In our own studies, we previously found 3 types of genes that show characteristically different expression patterns across the neocortical areas of adult macaques (Watakabe et al. 2006; Yamamori and Rockland 2006). 1) occ1, testican-1, testican-2, serotonin 1B, and serotonin 2A receptor genes exhibit enriched expression in the primate visual cortex (Tochitani et al. 2001; Takahata et al. 2008; Watakabe et al. 2008). 2) Growth/differentiation factor 7 is preferentially expressed in the primary motor area of the neocortex of African green monkeys (Watakabe, Fujita, et al. 2001). 3) Retinol-binding protein gene (*RBP*) is highly expressed in higher-order association areas of macaque neocortex (Komatsu et al. 2005). Interestingly, *RBP* mRNA distribution shows a highly layer-specific pattern. In the primary sensory areas, it is weak and restricted to layer II, but its expression increases toward the deeper layers along the ventral visual pathway. In the higher-order association areas, it is expressed widely in layers II–VI, except layer IV. Although the *RBP* gene is a good candidate to study the relationship between the structure and function of primate association areas, we think it is unlikely that *RBP* is the only gene that shows a pattern of association area–specific expression (Watakabe, Sugai, et al. 2001; Evans et al. 2003; Sato et al. 2007). It would help us to understand the features of association area–specific genes in primates if other genes with a comparable expression pattern could be identified and characterized.

We therefore performed additional rounds of screening for genes differentially expressed in adult macaque neocortical areas using a cDNA display method, namely, restriction landmark cDNA scanning (RLCS) (Suzuki et al. 1996; Shintani et al. 2004). By this method, we succeeded in identifying paraneoplastic antigen-like 5 gene (*PNMA5*) as a gene that is conspicuously and selectively expressed in primate association

areas. The *PNMA5* gene in humans is a member of a putative gene family that consists of 6 genes known as *PNMA1*, *PNMA2*, *PNMA3*, *PNMA4* (also called modulator of apoptosis-1, *MOAP1*), *PNMA5*, and *PNMA6A* (Schüller et al. 2005). The functions of this *PNMA* family of genes in the brain are unknown.

To understand the role of *PNMA5* and its gene family, we performed detailed expression analyses of these genes by in situ hybridization (ISH) in macaques, marmosets, and mice. We also performed northern blot hybridization and reverse transcription polymerase chain reaction (RT-PCR) in humans, African green monkeys, mice, and rats for gross expression analyses in these species. We found that *PNMA5* mRNA exhibited a pattern of area and laminar expression strikingly similar to that of *RBP* mRNA. Other family members were expressed in the macaque brains, but did not show such conspicuous area and laminar differences. Interestingly, among the *PNMA* family of gene, *PNMA5* and *PNMA1* were not expressed in the mouse brains. Comparisons between human and mouse sequences revealed moderate to high conservation in the amino acid sequences of *PNMA1*, *PNMA2*, *PNMA3*, and *MOAP1*, but considerable divergence of the sequences of *PNMA5* was observed. These results suggest an important role of *PNMA5* in the specialization of association areas during primate evolution.

Materials and Methods

Experimental Animals and Tissue Preparation

Three adult Japanese monkeys (*Macaca fuscata*) and 3 adult common marmosets (*Callithrix jacchus*) were used for histological analyses as previously reported (Takahata et al. 2006; Watakabe et al. 2007). Five adult mice (*Mus musculus*, C57BL/6, SLC, Japan) were also used. For tissue fixation, the mice were deeply anesthetized with Nembutal (100 mg/kg body weight, intraperitoneally) and perfused intracardially with 0.9% NaCl containing 2 U/mL heparin and then 4% paraformaldehyde in 0.1 M phosphate buffer at 4 °C. The brains were postfixed for 5 h at room temperature and then cryoprotected with 30% sucrose in 0.1 M phosphate buffer at 4 °C.

Adult African green monkeys (*Cercopithecus aethiops*; 1 female and 1 male for testis), adult mice (*M. musculus*, C57BL/6), and adult rats (*Rattus norvegicus*, Wistar) were used for northern blot hybridization and RT-PCR. The adult African green monkeys were used as previously reported (Watakabe, Fujita, et al. 2001). Mice and rats were deeply anesthetized with an overdose of Nembutal (100 mg/kg body weight, intraperitoneally) and sacrificed. All the experiments followed the animal care guidelines of the National Institute for Basic Biology and the National Institute for Physiological Sciences, Japan, and the National Institute of Health, United States.

RNA Isolation

Total RNAs were isolated from frozen tissues by the acid guanidinium thiocyanate–phenol–chloroform extraction method (Chomczynski and Sacchi 1987). Total RNA of a human brain was purchased from Clontech (Mountain View, CA). Poly(A) RNAs were purified from the total RNA using Oligotex-dT30 (TaKaRa, Otsu, Shiga, Japan) according to the manufacturer's recommended procedure.

RLCS Analysis

RLCS analyses were carried out essentially as described previously (Suzuki et al. 1996; Shintani et al. 2004), using poly(A) RNAs purified from 4 areas (area 46, primary motor area, temporal area, and primary visual area) of the African green monkeys. The double-stranded cDNAs were synthesized using the poly(A) RNA with a biotin-anchored primer and digested with a first restriction enzyme, *Bcl*I. The biotin-tagged fragments were radioisotope labeled. These fragments were collected and subjected to 1D agarose gel electrophoresis. After electrophoresis,

the cDNA fragments in the gel were again digested with a second restriction enzyme, *Hin*fI. The digested fragments were then subjected to 2D acrylamide gel electrophoresis.

The cDNA fragments separated in 2D electrophoresis were displayed as spots by autoradiography. A comparison of the intensity of each spot on the corresponding set of autoradiograms was performed, and cDNA spots showing different intensities among areas were eluted from the gel, subcloned, and their sequences determined.

In Situ Hybridization

For single-colored ISH, coronal sections were cut to 35-μm thickness. The digoxygenin (DIG)-labeled riboprobes were produced using template plasmids, which included the polymerase chain reaction (PCR) fragments generated using the primers listed in Supplementary Table S1. ISH was carried out as previously described (Liang et al. 2000; Komatsu et al. 2005). Briefly, free-floating sections were treated with proteinase K (5 μg/mL for macaque monkey and marmoset sections, and 1 μg/mL for mouse sections) for 30 min at 37 °C, acetylated, then incubated in a hybridization buffer (5× SSC, 2% blocking regent [Roche Diagnostics, Basel, Switzerland], 50% formamide, 0.1% *N*-lauroylsarcosine, 0.1% SDS) containing 0.5 μg/mL DIG-labeled riboprobes at 60 °C. The sections were sequentially treated in 2× SSC/50% formamide/0.1% *N*-lauroylsarcosine for 15 min at 60 °C twice, 30 min at 37 °C in RNase buffer (10 mM Tris-HCl [pH 8.0], 1 mM ethylenediaminetetraacetic acid [EDTA], 500 mM NaCl) containing 20 μg/mL RNase A (Sigma Aldrich, Saint Louis, MI), 15 min at 37 °C in 2× SSC/0.1% *N*-lauroylsarcosine twice, and 15 min at 37 °C in 0.2× SSC/0.1% *N*-lauroylsarcosine twice. The hybridization probe was detected with an alkaline phosphatase-conjugated anti-DIG antibody using DIG nucleic acid detection kit (Roche Diagnostics). For the ISH of *PNMA* family genes, 2 probes were prepared for each gene of 1 species. We confirmed that the 2 probes for each of the genes exhibited essentially the same hybridization signal patterns and there were no signals above the background with the sense probes. After confirming these points, the 2 probes were mixed together to intensify the signals.

Fluorescence double-colored ISH was carried out using DIG- and fluorescein-labeled riboprobes as described previously (Watakabe et al. 2007). The sections were cut to 15-μm thickness. The hybridization and washing were carried out as described above, except that both DIG- and fluorescein-labeled probes were used for the hybridization. After blocking in 1% blocking buffer (Roche Diagnostics) for 1 h, the probes were detected in 2 different ways. For the detection of fluorescein probes, the sections were incubated with an anti-fluorescein antibody conjugated with horseradish peroxidase (Roche Diagnostics, 1:2000 in the blocking buffer) for 3 h at room temperature. After washing in TNT buffer (0.1 M Tris–HCl [pH 7.5], 0.15 M NaCl, 0.1% Tween20) 3 times for 15 min, the sections were treated with 1:100-diluted TSA-Plus reagents (Perkin Elmer, Boston, MA) for 30 min according to the manufacturer's instruction, and the fluorescein signals were converted to dinitrophenol (DNP) signals. After washing with TNT buffer 3 times for 10 min, the sections were incubated overnight at 4 °C with an anti-DNP antibody conjugated with Alexa488 (1:500, Molecular Probes, Eugene, OR) in 1% blocking buffer for the fluorescence detection of the DNP signals. At this point, an anti-DIG antibody conjugated with alkaline phosphatase (1:1000, Roche Diagnostics) was also incubated for the detection of the DIG probes. The sections were washed 3 times in TNT buffer, once in TS 8.0 (0.1 M Tris–HCl [pH 8.0], 0.1 M NaCl, 50 mM MgCl₂), and the alkaline phosphatase activity was detected using HNPP fluorescence detection kit (Roche Diagnostics) according to the manufacturer's instruction. The incubation for this substrate was carried out for 30 min and stopped in PBS containing 10 mM EDTA. The sections were then counterstained with Hoechst 33342 (Molecular Probes) diluted in PBS to 1:1000 for 5 min. All the figures obtained in the ISH experiments were adjusted for appropriate contrast using Adobe Photoshop (Adobe Systems Inc., San Jose, CA).

Quantification of ISH Signals

We analyzed the optical densities of the ISH signals of *PNMA5* and *RBP* mRNAs to investigate the layer distribution. First, the layer borders

were determined based on the Nissl staining patterns of the adjacent sections. The images of the ISH-stained sections of *PNMA5* and *RBP* were then transformed using Adobe Photoshop, so that the heights of the images became equal. The optical density of the adjusted images was measured using ImageJ image analysis software (Abramoff et al. 2004) after binarization of the signals with an equable criterion, mean minus standard deviation (SD) in the gray scale image.

Furthermore, we manually counted the double positive cells for *PNMA5* mRNA and either one of the *VGLUT1*, *GAD67* or *RBP* mRNAs. For the counting, 15-μm-thick sections containing several areas were used for the double ISH. These areas were identified in reference to a standard atlas (Paxinos et al. 1999). The following procedures were carried out using Adobe Photoshop. The images taken in 3 channels (ISH signals in red/green channels and Hoechst nuclear staining in the blue channels) were layered into a single file. Eight 200 × 200 μm² windows were selected within layer II and upper region of layer III of each area for counting. On the basis of Hoechst staining, the cells positive for red or green ISH fluorescent signals were plotted manually onto a blank layer as dots for later counting. The numbers and proportions of double positive cells for *PNMA5* mRNA and 1 of *VGLUT1*, *GAD67* or *RBP* mRNAs were counted, and then calculated for each window of each area and averaged.

Northern Blot Hybridization and RT-PCR

Northern blot hybridization was carried out essentially as described previously (Sambrook et al. 1989). Briefly, glyoxylated poly(A) RNA was electrophoresed in 1.2% agarose gel and transferred onto a Hybond N+ nylon membrane (GE Healthcare, Little Chalfont, Buckinghamshire, England). For each probe, regions between the primers listed in Supplementary Table S1 were labeled with ^{32}P by random priming. After 2 h of prehybridization in a hybridization buffer (50 mM Tris–HCl [pH 7.5], 10 mM EDTA [pH 8.0], 1% sodium *N*-dodecanoyl salcosinate, 1 M NaCl, 0.2% bovine serum albumin, 0.2% ficoll 400, 0.2% polyvinylpyrrolidone, 100 μg/mL salmon sperm DNA), ^{32}P-labeled probes were added to a final concentration of 5 × 10^5 cpm/mL. Hybridization was carried out at 65 °C overnight. After hybridization, the membrane was washed twice in 0.2× SSC (16.65 mM NaCl, 16.65 mM trisodium citrate dihydrate) with 0.1% sodium dodecyl sulfate (SDS) and autoradiographed. The membrane blotted with the mRNAs of the African green monkeys was used in the previous report (Watakabe, Fujita, et al. 2001). For RT-PCR, 1.0 μg of DNase-treated total RNA was reverse-transcribed using Superscript II RNase H⁻ Reverse Transcriptase (Invitrogen, Carlsbad, CA). After the reaction was terminated, the reaction mixtures were diluted 2-fold with distilled water. PCR was performed in 10 μL of reaction mixtures, containing 1 μL of the reaction mixture, 2 pmol of gene-specific primers (Supplementary Table S1), 1× KOD-Plus buffer, 2 nmol each of dNTP, 10 nmol MgSO$_4$, 5% DMSO and 0.2 units of KOD-Plus polymerase (TOYOBO, Osaka, Japan). An initial denaturation step of 5 min at 95 °C was followed by predetermined optimal cycles of 94 °C for 30 s, 55 °C for 30 s, and 68 °C for 40 s. PCR products obtained with the same primer set for RNAs derived from different tissues were loaded and separated on the same 1% agarose gel and visualized with ethidium bromide.

Sequence Determination of PNMA5 and the PNMA Family Genes

We cloned cDNAs of all known *PNMA* family genes in the human, African green monkey, and mouse and determined their nucleotide sequences. For the African green monkey, library screening and isolation of positive clones were carried out according to the standard screening procedure. The cDNA inserts of the positive clones were recovered in the form of plasmids by in vivo excision. All the cDNAs were considered to contain the full coding regions because we found a stop codon in the frame upstream from the putative initiation methionine codon for each cDNA. We did not succeed in isolating positive clones for *PNMA6A* cDNA in the African green monkey and mouse. For the human and the mouse, we designed the gene-specific primers from the NCBI database (Supplementary Table S1), and the cDNAs of *PNMA* family genes were amplified by RT-PCR using brain or testis mRNA as templates.

Results

Identification of PNMA5 as an Association Area–Specific Gene

For a systematic large-scale screening of area-specific genes in the adult macaque neocortex, we carried out RLCS (Suzuki et al. 1996; Shintani et al. 2004) using mRNAs purified from 4 distinct cortical areas (area 46, primary motor, temporal, and primary visual areas; Fig. 1*A*) as described in the Materials and Methods section. Using a pair of the restriction enzymes of *Bcl*I and *Hin*fI, we found several spots showing different expression profiles among neocortical areas. One of these spots was most abundant in the association areas of the frontal (area 46) and temporal areas but was almost absent in the visual area (Fig. 1*C*). This spot was excised from the gel, and the corresponding gene was identified as *PNMA5*. RT-PCR analysis confirmed the area-specific expression of *PNAM5* mRNA (data not shown).

Distribution of PNMA5 mRNA in the Macaque Brain

To examine the distribution of *PNMA5* mRNA in detail, we carried out ISH using adult macaque brains. Figure 2 shows the distribution patterns of *PNMA5* mRNA in various coronal sections. Overall, the cortical expression of *PNMA5* mRNA was high and the expressions in the subcortical nuclei were low. Consistent with the results of the RLCS analysis, we observed a heterogeneous expression pattern within the neocortex: That is, we observed strong expression in the prefrontal (Fig. 2*A*, area 46) and temporal association areas (Fig. 2*D*, TE), whereas we observed weak expression in the occipital cortex. It was particularly weak in the primary visual area (Fig. 2*G*, V1). In addition to the neocortical areas, strong expression was observed in the limbic regions such as the insular (Fig. 2*C*), cingulate (Fig. 2*C*), perirhinal (Fig. 2*D*), and entorhinal cortices (Fig. 2*D*), as well as the amygdala (Fig. 2*C*) and hippocampus (Fig. 2*E*).

The expression patterns of *PNMA5* mRNA showed area-specific differences within layers (Fig. 3). In the frontal association areas such as area 46 (Fig. 3*A*), strong *PNMA5* mRNA expression was observed throughout layers II–VI, with dense staining in layer II, but low expression in layer IV. In the temporal association areas such as TE (Fig. 3*H*), perirhinal (Fig. 3*I*) and entorhinal cortices (Fig. 3*J*), strong *PNMA5* mRNA expression was observed (see below). In contrast, *PNMA5* mRNA expression was weak and mainly restricted to layer II in the primary sensory areas such as the primary auditory (Fig. 3*C*, A1), somatosensory (Fig. 3*D*, area 3b), and visual (Fig. 3*E*, V1) areas. In the primary motor area (Fig. 3*B*, area 4), the *PNMA5* mRNA signals were mainly located in layer II as in the primary sensory areas. However, sparse signals were also present in layers III and V. Along the ventral visual pathway toward higher-order areas, we observed gradual increases of *PNMA5* mRNA expression in both of the intensity and laminar distribution. In V1 (Fig. 3*E*), *PNMA5* mRNA expression was restricted mainly to a narrow layer at the top of layer II as described earlier. However, in V2 (Fig. 3*F*), its expression extended over the entire layer II, but still restricted only within the supragranular layer. In V4 (Fig. 3*G*), *PNMA5* mRNA expression was also observed predominantly in layer II, but weakly detected in layers III, V, and VI as well. In TE (Fig. 3*H*), the *PNMA5* mRNA expression in layers III, V, and VI was stronger than that in V4, but absent in layer IV. In the
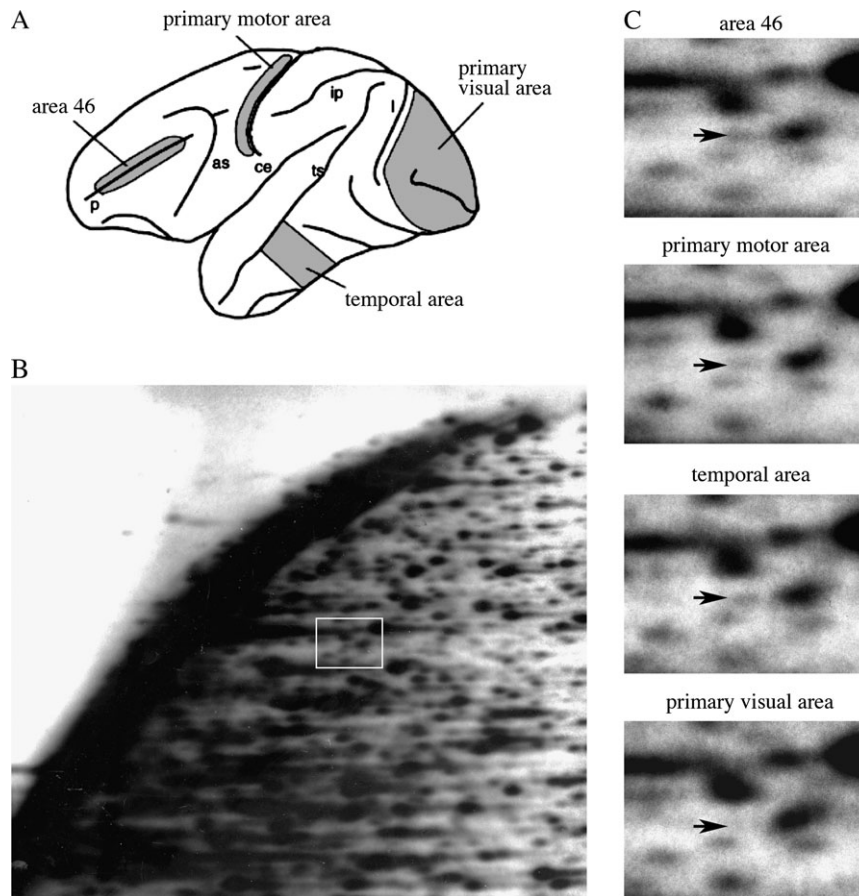
Figure 1. Identification of *PNMA5* as a gene preferentially expressed in the association areas. (*A*) The left hemisphere of the macaque neocortical areas is illustrated. Anterior is to the left and posterior to the right. Major sulci are indicated by lower case letters: p, principal sulcus; as, arcuate sulcus; ce, central sulcus; ip, intraparietal sulcus; ts, superior temporal sulcus; l, lunate sulcus. (*B*) RLCS analysis of the macaque neocortex. This panel shows an example of an autoradiography of a 2D gel of RLCS analysis in area 46, digested with *Bcl*I and *Hinf*I. Four distinct regions of the macaque neocortex depicted in panel *A* were analyzed. The area corresponding to the white box is shown at higher magnification in panel *C*. (*C*) Higher magnification of the boxed region in panel *B* in 4 distinct areas of panel *A*. Arrows indicate the spot of *PNMA5* mRNA. These spots were strong in area 46 and temporal area, and relatively weak in the primary motor and lowest in the primary visual area.

perirhinal cortex (Fig. 3*I*), *PNMA5* mRNA was strongly expressed in layers II and V with no expression in layer IV. In the entorhinal cortex (Fig. 3*J*), *PNMA5* mRNA expression was strongly observed in all the layers. In the hippocampus (Fig. 3*K*), *PNMA5* mRNA was expressed through CA1–CA4 and the dentate gyrus except that the expression was low in CA2 and absent in the Subiculum.

In summary, *PNMA5* mRNA showed strong expression in layers II, III, V, and VI of the association areas and in the limbic regions, but was weak and restricted only to layer II in the primary sensory areas and subcortical nuclei in macaque brains.

PNMA5-*mRNA-Positive Cells Are Mostly Excitatory Neurons*

To determine the type of cells that express *PNMA5* mRNA, we examined what percentages of excitatory and inhibitory neurons express *PNMA5* mRNA. For this purpose, we performed double ISH of *PNMA5* mRNA with either vesicular glutamate transporter 1 (*VGLUT1*) mRNA as a glutamatergic excitatory neuronal marker (Takamori et al. 2000) or glutamate decarboxylase 1 (*GAD67*) mRNA as a GABAergic inhibitory neuronal marker. Figure 4 shows a typical example of such double ISH in area TE. At a first glance, it was clear that most cells that expressed *PNMA5* mRNA also coexpressed *VGLUT1*

mRNA (Fig. 4*A*, lower panels for coexpression). In our counting, over 95% of the *PNMA5*-mRNA-positive neurons coexpressed *VGLUT1* mRNA in layer II (Table 1). Conversely, most of the excitatory neurons in layer II (ca. 70%) expressed *PNMA5* mRNA in area 9, area 4 and TE (Table 1). On the other hand, we observed little coexpression of *PNMA5* mRNA with *GAD67* mRNAs (Fig. 4*B*, lower panels for coexpression). Less than 4% of the *PNMA5*-mRNA-positive neurons expressed *GAD67* mRNA (Table 1). It is also worth noting that the expression of *PNMA5* mRNA per cell varied consecutively from undetectable to abundant levels and not in all-or-none fashion. In the deeper layers and in the primary sensory areas, *PNMA5* mRNAs showed generally low levels of expressions even in the positive cells.

Distribution of PNMA5 *mRNA Is Similar to That of* RBP *mRNA*

The distribution of *PNMA5* mRNA in the adult macaque brains as mentioned above was strikingly similar to that of *RBP* mRNA (Komatsu et al. 2005). Thus, we directly compared expressions of *PNMA5* and *RBP* mRNAs in the adjacent sections. As shown in Figure 5*A*, the overall expression patterns of the 2 mRNAs in the adult brain were very similar (Fig. 5*A*). Both the mRNAs showed strong expressions in the
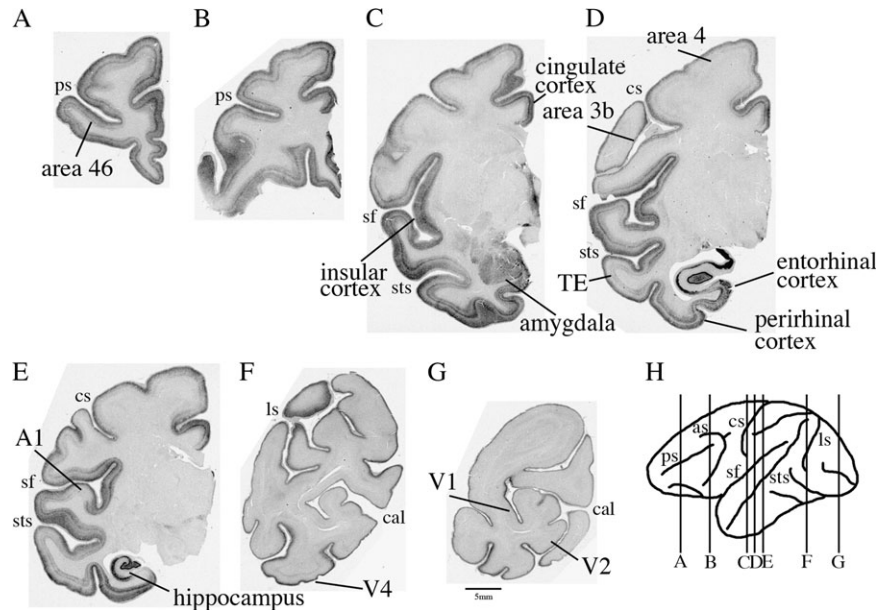
Figure 2. Distribution of *PNMA5* mRNA in macaque brains. Coronal sections were prepared from the positions depicted on the brain diagram in *H* as *A–G*, and *PNMA5* mRNA was detected by ISH. This figure is comprised of the sections from 3 macaques. Panel *C* is from 1 macaque, panel *E* is from another one, and the other panels are from a third macaque. Some of the representative areas magnified in Figure 3 are shown. Abbreviations: ps, principal sulcus; as, arcuate sulcus; ce, central sulcus; sf, sylvian fissure; sts, superior temporal sulcus; ls, lunate sulcus; cal, calcarin sulcus.

frontal (Fig. 5*A1*, area 46) and the temporal association areas (Fig. 5*A3*, TE), cingulate (Fig. 5*A2*), insular (Fig. 5*A2*), perirhinal (Fig. 5*A3*), and entorhinal cortices (Fig. 5*A3*) as well as the amygdala (Fig. 5*A2*) and hippocampus (Fig. 5*A4*), but showed weak expressions in the primary sensory areas such as A1 (Fig. 5*A4*), area 3b (Fig. 5*A3*), and V1 (Fig. 5*A5*), as well as most subcortical nuclei.

Besides such fundamental similarities, we also observed several differences between the expression patterns of the 2 genes. For example, in the association areas, the expression level of *PNMA5* mRNA in layer III was substantially lower than that of *RBP* mRNA (Fig. 5*B*, area 46 and TE). We also observed that the expression of *PNMA5* mRNA in layer V was slightly higher than that of *RBP* mRNA (Fig. 5*B*, area 46 and TE). In the entorhinal cortex, *PNMA5* mRNA was expressed strongly in all the layers, but *RBP* mRNA was not expressed in layer VI (Komatsu et al. 2005). To confirm the similarity of the expressions at the cellular level, we performed double ISH of *PNMA5* and *RBP* mRNAs. The vast majority of the cells that express *PNMA5* mRNA coexpressed *RBP* mRNA in layer II (over 95%, Fig. 5*C* and Table 1). The number of cells that express *RBP* mRNA was greater than the number of cells that express *PNMA5* mRNA by approximately 30% on average (Table 1). Thus, some excitatory neurons in layer II seemed to express only *RBP* mRNA, whereas other neurons coexpressed both mRNAs. In the deeper layers and in the primary sensory areas, both mRNAs showed generally low levels of expressions and concentration, and not necessarily confined to particular subpopulations for either mRNA.

We note that this similarity of expression was limited to the brain. The northern blot hybridization analysis of various organs showed that the mRNAs of *PNMA5* and *RBP* showed quite different expression patterns. *RBP* mRNA was expressed more in the liver than brain (Pfeffer et al. 2004). The mRNA expression of *PNMA5* was restricted only to the brain and

testis, whereas *RBP* mRNA was expressed in several other tissues (Supplementary Fig. S1 and see below).

Comparative Analyses of PNMA5 *and the Putative Family Genes*

PNMA1, *PNMA2*, *PNMA3*, *MOAP1* (*PNMA4*), *PNMA5*, and *PNMA6A* genes are considered to form a gene family (Schüller et al. 2005). The amino acid identities between these family genes range from 38.5% (between *PNMA5* and *PNMA6A*) to 56.6% (between *PNMA1* and *MOAP1*) (Supplementary Table S2). The percent identity of the amino acid sequences of *PNMA5* between the human and mouse was low (57.0%), although that of *PNMA1* was highly conserved (92.1%), and those of *PNMA2*, *PNMA3* and *MOAP1* were moderately conserved (78.7%, 74.5%, and 77.1%, respectively) (Table 2). The low conservation of *PNMA5* sequence led us to determine the sequences of *PNMA* family genes in the African green monkey. The amino acid sequence identity between human and African green monkey *PNMA5* was 93.6% (Table 2). This was substantially lower than those of the other *PNMA* family genes (99.7%, 97.8%, 98.3%, and 97.4%, respectively).

Next, we examined the mRNA expression patterns of *PNMA* family genes in several tissues from the African green monkeys and mice by northern blot hybridization (Fig. 6*A,C*). In the African green monkeys, *PNMA5* mRNA was expressed specifically in the neocortex and testis (Fig. 6*A*). In the neocortex, *PNMA5* mRNA was strongly expressed in the temporal area and area 46, but weakly in the primary sensory areas, particularly in the primary visual area, which is consistent with the results of the RLCS analysis and ISH (Fig. 6*A*). The densitometric quantification showed that the *PNMA5* mRNA expression level in the temporal area or area 46 was approximately 4-fold higher than that in the primary visual area (Fig. 6*B*). We also detected strong expressions of *PNMA1*, *PNMA2*, *PNMA3*, and *MOAP1* mRNAs in the neocortex (Fig. 6*A*). However, the mRNA
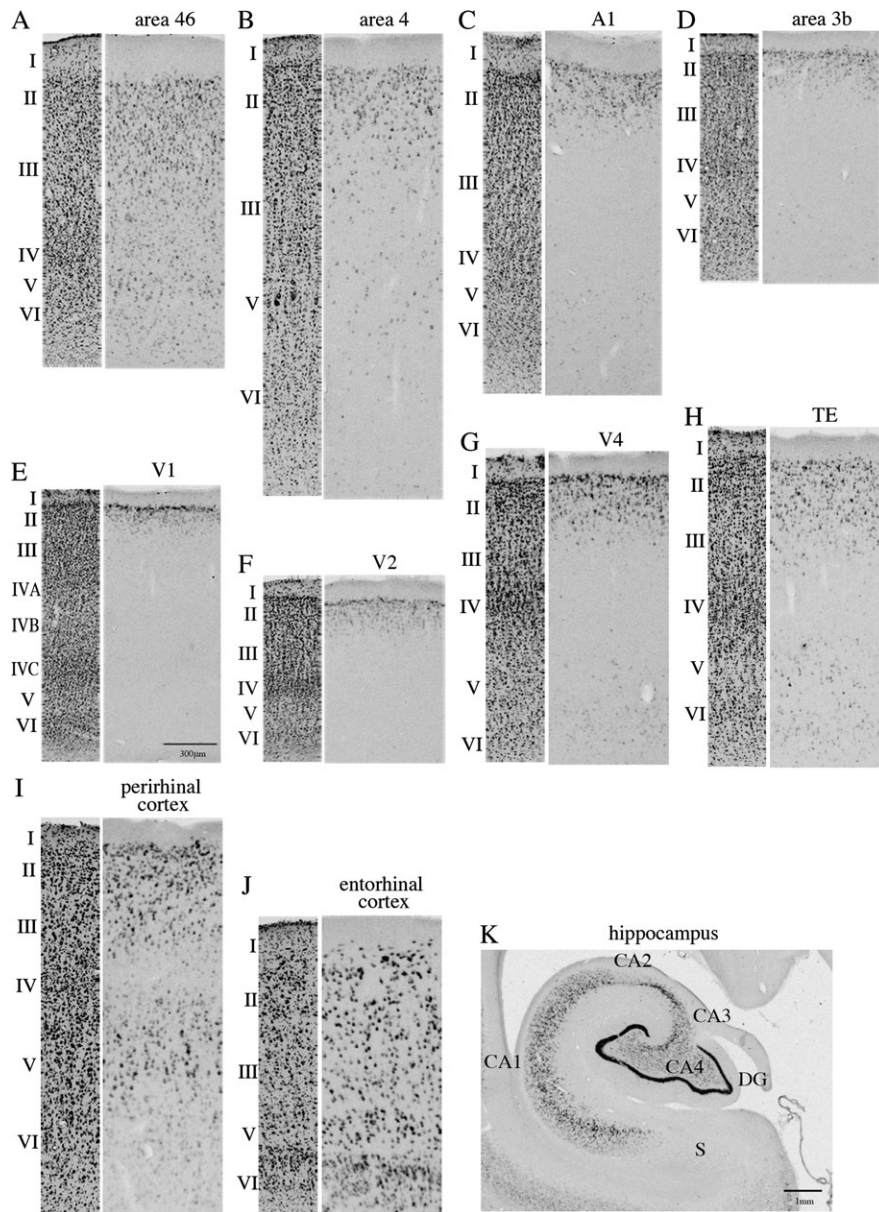
Figure 3. Expression pattern of *PNMA5* mRNA in the macaque cortex. The cortical areas and hippocampus depicted in Figure 2 are magnified. The layers indicated on the left side of each panel were identified according to the Nissl staining of the nearby section. Left of each panel shows Nissl staining and right shows the expression patterns of *PNMA5* mRNA by ISH. Abbreviations: DG, dentate gyrus; S, subiculum.

expression levels of each gene in the neocortical areas were similar (Fig. 6*B*). In addition to the neocortex, these 4 genes were expressed in the cerebellum and spinal cord as well. The mRNAs of *PNMA1* and *PNMA3* were also expressed in other tissues (Fig. 6*A*). *PNMA1* mRNA showed ubiquitous expressions, although the levels of expressions among the tissues were different. *PNMA3* mRNA was expressed in the testis.

We next examined the mRNA expressions of the *PNMA* family genes in the mouse tissues by northern blot hybridization and RT-PCR. Interestingly, we found that the expression patterns in the tissues of mice were quite different from those of the African green monkeys. First, *PNMA5* mRNA was detected at a low level only in the testis of mice, and in no other tissues including the brain (Fig. 6*C*). This expression pattern was confirmed by RT-PCR (Fig. 6*D*). The RT-PCR

experiments also showed that *PNMA5* mRNA was not expressed in the brain at any developmental stage tested. Also in rats, *PNMA5* mRNA expression was confirmed in the testis, but not in the brain (Fig. 6*E*). Second, in contrast to the widespread expression of *PNMA1* mRNA in the tissues of the African green monkeys, it was detected only in the testis of the mice. Third, *PNMA3* mRNA was not detected in the mouse testis, whereas *MOAP1* mRNA was strongly expressed. In addition, the expression of *MOAP1* mRNA in the mouse was relatively ubiquitous, the pattern of which was similar to that of *PNMA1* mRNA in the African green monkey.

In addition to the 5 *PNMA* family genes described above, the *PNMA6A* gene is annotated in the human genome. We confirmed its mRNA expression in the human brain by RT-PCR (Fig. 6*F*). In the human genome, the *PNMA6A* gene is
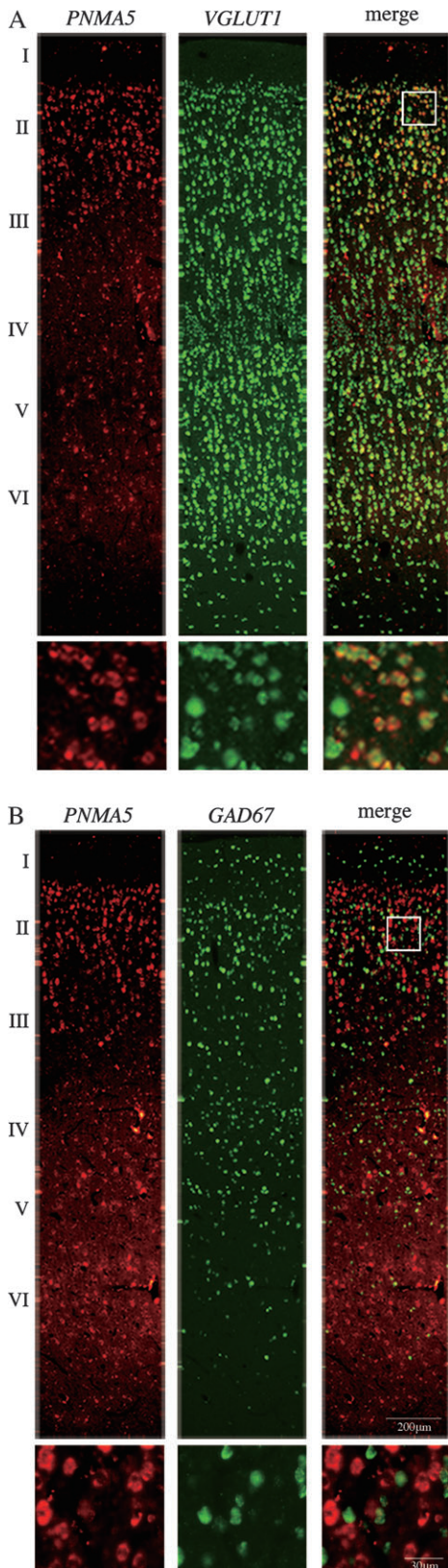
Figure 4. Double ISH of *PNMA5* and *VGLUT1* or *GAD67* mRNAs in area TE. (*A*) *PNMA5* mRNA (left, red) was expressed in most of the *VGLUT1*-mRNA-positive cells (middle, green) in layer II (bottom: higher magnification). (*B*) *PNMA5* mRNA was barely expressed in *GAD67*-mRNA-positive cells (middle, green).

located next to *PNMA3* gene, and they are separated by approximately 12 kb. There is also a very similar *PNMA6B* gene (99.2% amino acid identity), which is separated by 0.6 kb from the *PNMA6A* gene and positions in the reverse orientation. However, *PNMA6A* gene orthologue is not present in the corresponding location in the mouse genome compilation of the NCBI database. Furthermore, we could not clone the *PNMA6A* gene fragments of either macaque or mouse by either RT-PCR or genomic PCR. By southern blot hybridization, we detected clear hybridizing bands for *PNMA6A* in the human and slowloris (prosimian) genomes, but not in the African green monkey (Old World monkey) and common marmoset (New World monkey) genomes (data not shown). Thus, although *PNMA6A* gene could be functional in humans, it appears to be absent in macaques, and we therefore refrained from further investigation.

Expression Patterns of PNMA *Family Genes in Monkeys and Mice*

To examine the distribution of the mRNAs of *PNMA* family genes in more detail, we carried out ISH. Figure 7 shows the mRNA expression patterns of 4 *PNMA* family genes in the adult macaque neocortex. In the macaque neocortex, the mRNAs of the 4 genes were observed in all the areas and layers examined, although the layers where these genes were preferentially expressed slightly differed from each other. The differential expressions of these genes were most notable in V1. In V1, *PNMA1* mRNA showed a relatively weak expression below layer IVC and was particularly weak in layer V. On the other hand, *PNMA2* mRNA showed relatively weak signals in layer IVC. *PNMA3* and *MOAP1* mRNAs showed patterns similar to that of *PNMA1* mRNA, although the signal intensities of these 2 genes were weaker than that of *PNMA1* mRNA. In the other primary sensory areas, such as area 3b, *PNMA3* mRNA seemed to be expressed strongly in the upper layers than lower layers. This was also observed in the primary auditory area (data not shown). In the subcortical regions, we observed relatively ubiquitous expressions of the 4 mRNAs. However, *PNMA3* mRNA was expressed only in sparsely distributed cells of the caudate nucleus (Fig. 7*A*).

To determine the cell types that express these mRNAs in the neocortex, we performed double ISH of each of these genes with *VGLUT1* or *GAD67* mRNAs. Unlike *PNMA5* mRNA, the mRNAs of these 4 family genes were all colocalized with both *VGLUT1* and *GAD67* mRNAs (Supplementary Fig. S2). Thus, these genes appear to be expressed in almost all the neurons in the neocortical areas, although the expression levels per cell varied.

We next examined the mRNA expressions of *PNMA* family genes in the mouse brain by ISH (Fig. 8). In our analysis, *PNMA5* and *PNMA1* mRNAs were poorly expressed in any part of the mouse brains, the results of which were consistent with those of northern blot hybridization. No *PNMA5* mRNA was expressed anywhere in the brain, whereas the *PNMA1* mRNA was observed at a very low level in the piriform cortex, hippocampus and some subcortical nuclei. *PNMA2*, *PNMA3*, and *MOAP1* mRNAs were abundantly expressed in the mouse brain. In the neocortex, *PNMA2*, *PNMA3*, and *MOAP1* mRNAs were expressed throughout all the layers, although the expression levels of the genes differed slightly among the layers (Fig. 8*B*). For example, the expression level of *PNMA2*

Table 1

Number of neurons positive for *PNMA5* or neuron marker genes in layer II

	PNMA5		*VGLUT1*		Double positive[a] (number)	Double positive[a] /*PNMA5* (%)	Double positive[a] /*VGLUT1* (%)
	Number	Density	Number	Density			
Area 9	23.4 ± 3.2	39.0 ± 5.3	29.3 ± 3.2	48.8 ± 5.3	22.6 ± 3.2	96.9 ± 4.3	77.2 ± 4.0
Area 4	29.3 ± 5.1	48.8 ± 8.4	42.0 ± 8.1	70.0 ± 13.5	28.0 ± 5.3	95.5 ± 2.8	67.3 ± 8.4
TE	33.1 ± 7.0	55.2 ± 11.7	48.1 ± 9.0	80.2 ± 15.0	31.8 ± 7.1	95.7 ± 3.4	65.8 ± 6.1

	PNMA5		*GAD67*		Double positive[b] (number)	Double positive[b] /*PNMA5* (%)	Double positive[b] /*GAD67* (%)
	Number	Density	Number	Density			
Area 9	24.3 ± 5.0	40.4 ± 8.3	14.6 ± 3.4	24.4 ± 5.7	0.4 ± 0.5	1.6 ± 2.2	2.5 ± 3.6
Area 4	23.4 ± 5.1	39.0 ± 8.5	16.5 ± 4.6	27.5 ± 7.7	0.5 ± 0.8	2.2 ± 3.2	2.6 ± 3.7
TE	45.0 ± 16.7	75.0 ± 27.8	29.4 ± 7.5	49.0 ± 12.6	1.8 ± 1.4	4.0 ± 3.1	5.9 ± 4.6

	PNMA5		*RBP*		Double positive[c] (number)	Double positive[c] /*PNMA5* (%)	Double positive[c] /*RBP* (%)
	Number	Density	Number	Density			
Area 9	23.1 ± 5.6	38.5 ± 9.3	27.9 ± 6.2	46.5 ± 10.3	22.9 ± 5.8	98.7 ± 2.5	82.0 ± 9.3
Area 4	17.6 ± 8.5	29.4 ± 14.1	24.3 ± 8.2	40.4 ± 13.7	17.3 ± 8.6	97.2 ± 4.2	68.6 ± 17.0
TE	29.2 ± 7.5	48.8 ± 13.6	36.2 ± 7.4	60.0 ± 12.0	27.7 ± 6.9	95.0 ± 3.3	76.1 ± 7.0

Numbers of layer II neurons positive for *PNMA5*, *VGLUT1*, *GAD67*, and *RBP* mRNAs in area 9, area 4, and TE of a macaque are shown.

Number: the numbers of positive neurons in 200 × 200 μm^2 window are shown for layer II of each area.

The mean ± SD was calculated from the counts of 8 independent windows in each area.

Density: the density of the positive neurons per mm^3 of tissue (in thousands) ± SD.

[a] The means ± SD of the number of *PNMA5* and *VGLUT1* double positive neurons.

[b] The means ± SD of the number of *PNMA5* and *GAD67* double positive neurons.

[c] The means ± SD of the number of *PNMA5* and *RBP* double positive neurons.

mRNA was low in layer IV. Although the expression of *PNMA3* mRNA was strong in the upper layers but relatively weak in the lower layers, that of *MOAP1* mRNA was strong in layer V. In the subcortical regions, *PNMA2* mRNA was expressed in the striatum and hypothalamus, but was relatively weak in the thalamus. *PNMA3* mRNA was expressed weakly in the striatum but strongly in the hypothalamus. *MOAP1* mRNA was expressed weakly in the striatum but strongly in the thalamus and hypothalamus. The mRNA expression patterns of *PNMA2*, *PNMA3*, and *MOAP1* in the brain of macaques and mice were basically conserved.

The different expression patterns of *PNMA5* and *PNMA1* mRNAs between macaques and mice raised an interesting possibility that the expression of the 2 genes may be primate specific. To test this, we examined the expressions of all *PNMA* family genes including *PNMA5* in the neocortex of marmosets, which belong to the New World monkey that is of different lineage from the Old World monkey including macaques. In the marmosets, the expression patterns of these 5 *PNMA* genes showed similarity to those in the macaques (Supplementary Fig. S3). *PNMA5* mRNA showed area-specific expression patterns similar to those in the macaques: It was strong in the frontal and temporal association cortices and weak in the parietal and occipital cortices. The mRNAs of the other *PNMA* family genes were expressed in all the areas and layers, although the expression levels of the genes differed among the layers, particularly in the occipital cortex (V1). These expression patterns of the *PNMA* family genes in marmosets were all similar to those in the macaques.

Discussion

In this study, we have identified a novel gene, *PNMA5*, whose transcript is preferentially expressed in the primate association areas. The expression pattern of *PNMA5* mRNA in the macaque

neocortex was similar to that of *RBP* mRNA, which we previously reported as being enriched in the excitatory neurons of association areas (Komatsu et al. 2005). The very similar expression patterns of the *PNMA5* and *RBP* genes suggest that these 2 genes have roles in closely related cortical circuits, which may well be involved in fundamentally associative functions of the neocortex. The comparative expression analyses showed that *PNMA5* mRNA is expressed in the primate brains (macaques and marmosets), but not in mouse brains. The sequence comparison indicated that the *PNMA5* sequences among mammals are significantly diverged even within primates. Divergences in the amino acid sequences and mRNA expression of *PNMA5* suggest that it acquired a specialized role in the association areas of neocortex during primate evolution.

Common Laminar Pattern for PNMA5 and RBP mRNA Expressions

The expression patterns of *PNMA5* and *RBP* mRNAs were very similar in terms of laminar specificity across areas of the macaque neocortex. One common feature is that *PNMA5* and *RBP* mRNAs were expressed in layer II across neocortical areas including V1. As we discussed previously (Komatsu et al. 2005), several lines of evidence suggest a specialized role, possibly related to integration, for layer II in the macaques. For example, the neurons in layer II generally receive the convergence of several feedback cortical inputs (Kennedy and Bullier 1985; Rockland and Virga 1989; Rockland et al. 1994), as well as amygdalo–cortical projections (Freese and Amaral 2005). Physiologically, there are cells near the border between blob and interblob regions in layers II and III that have mixed receptive field properties (Nealey and Maunsell 1994). Shipp and Zeki (2002) indicate that the responses for visual stimuli in layer II of V2 are generalized for directional, orientational and
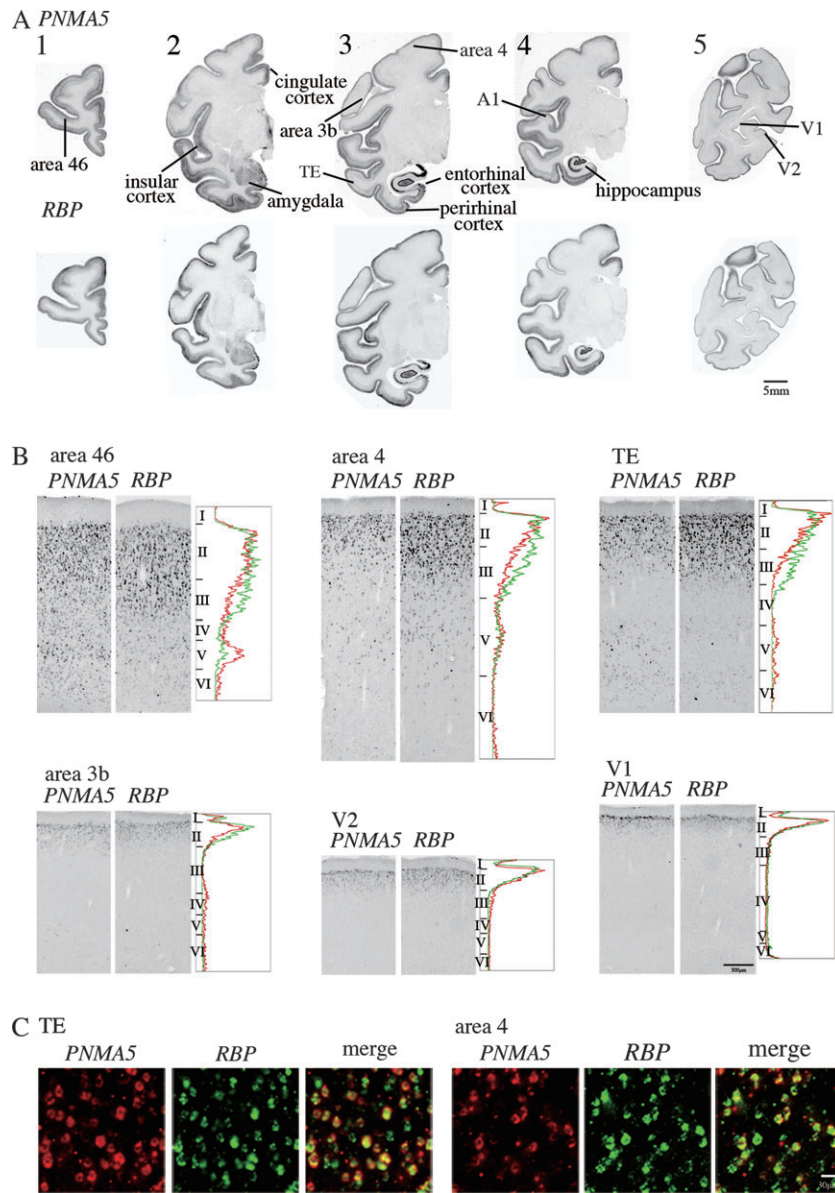
Figure 5. Comparison of expression patterns of *PNMA5* and *RBP* mRNAs in macaque brains. (*A*) Coronal sections at positions *A*, *C*, *D*, *E*, and *F* in Figure 2 are shown. (*B*) Higher magnification views of several areas. The expression patterns of *PNMA5* and *RBP* mRNAs are shown, together with the laminar profiles of ISH signals quantified by measuring the optical density (red, *PNMA5* mRNA; green, *RBP* mRNA). These profiles show the averages of the normalized values of 2 or 3 different macaques. The cortical layers were identified in reference to the Nissl staining of the nearby section. (*C*) Double ISH of *PNMA5* and *RBP* mRNAs were performed to examine the coexpression of these mRNAs. Note that *PNMA5* mRNA (left, red) is expressed in a large population of *RBP*-mRNA-positive cells (middle, green) in layer II.

spectral sensitivities, and speculate that multimodal association neurons in layer II induce sets of functionally unimodal projection neurons to adopt correlated rates of firing. There is, thus, a possibility that both *PNMA5* and *RBP* contribute to specifically associative properties of layer II neurons. Several studies have shown that layer II neurons are contributing to feedback projections, whereas neurons in the deeper part of the supragranular layers (layer III) are associated with feedforward projections in visual areas (Tigges et al. 1973; Kennedy and Bullier 1985). Physiological differences are reported between the neurons in layer II and layer III of the primary visual cortex of macaque monkeys (Gur and Snodderly 2008). This observation may be related to the theory that layer III neurons are involved in generating and transmitting

information about image features, whereas layer II neurons may participate in top-down influences from higher cortical areas (Ullman 1995). Connectionally and physiologically different properties of layer II and III neurons in visual areas may be reflected in the expression of *PNMA5* and *RBP* in the occipital areas where they are expressed only in the upper part of the supragranular layers.

A second shared feature is the laminar expansion of *PNMA5* and *RBP* mRNAs from superficial to deeper layers, which occurs gradually from the primary sensory areas to higher-order association areas. Elston and coworkers reported that there exists a gradient across areas for dendrite architectures of pyramidal neurons in layer III (Elston et al. 1999; Elston 2000); that is, the size of the basal dendritic field and the spine

Table 2

Comparison of amino acid and nucleotide sequences of human with those of other species

		AGM	Mouse
PNMA5	% a.a.	93.6	57.0
	% nuc.	96.0	70.4
PNMA1	% a.a.	99.7	92.1
	% nuc.	98.8	87.4
PNMA2	% a.a.	97.8	78.7
	% nuc.	98.0	78.3
PNMA3	% a.a.	98.3	74.5
	% nuc.	98.1	80.3
MOAP1	% a.a.	97.4	77.1
	% nuc.	97.8	80.6
PNMA6A	% a.a.	ND	ND
	% nuc.	ND	ND

AGM: African green monkey.
% a.a.: percent identity of amino acid sequences.
% nuc.: percent identity of nucleotide sequences.
ND: not determined.

density increase in the association areas, which they interpret as signifying differential associative capacities. Interestingly, there are other reports of gradientwise changes, for example, changes in cross-sectional areas of patchy intrinsic terminations along the ventral visual pathway, which are interpreted as reflecting the increase of global computational roles (Amir et al. 1993; Lund et al. 1993; Tanigawa et al. 2005). These observations support the possibility that associative processes gradually occupy more neural space with progression along the sensory pathways. We propose that *PNMA5* and *RBP* are generally involved in associative processes in layer II throughout all layers, but that their role is only gradually extended to other layers in the higher-order association areas.

Third, recent studies in macaques show that the laminar distribution and of synaptic zinc in the occipito-temporal pathway is very similar to those of the *PNMA5* and *RBP* mRNAs. That is, synaptic zinc is very poor in layer IV, but in anterior
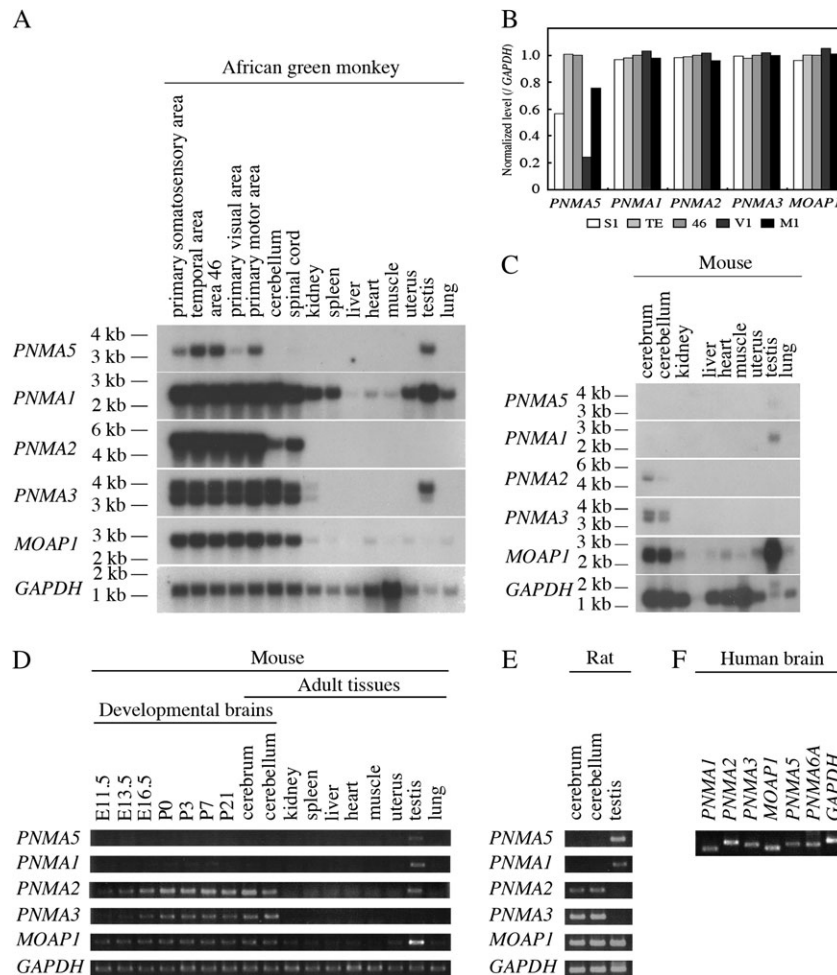
Figure 6. Expression analyses of *PNMA5* gene and the *PNMA* family genes in various tissues by northern hybridization and RT-PCR. (*A,C*) Northern hybridization of *PNMA* family genes of African green monkeys (*A*) and mice (*C*). A single membrane blotted with various poly(A) mRNAs was serially probed with 5 *PNMA* family genes and *GAPDH* gene with repeated stripping and hybridization. No hybridization signals were detected after each stripping. The positions of the size marker are indicated on the left. (*B*) Quantification of northern hybridization in the neocortical areas of the African green monkey. The X-ray films shown in panel *A* were scanned and digitized for quantification. This panel shows the results of quantification of the lanes for 5 neocortical areas of the African green monkey for each gene. The expression levels were normalized to the ratio between the *PNMA* and *GAPDH* mRNA expression levels in area 46. The expression levels of *PNMA3* mRNA are indicated by the averages of the upper and lower bands. Abbreviations: S1, primary somatosensory area; TE, temporal area; 46, area 46; V1, primary visual area; M1, primary motor area. (*D–F*) RT-PCR analyses of the *PNMA* family genes expressed in developmental brains and various adult tissues of mice (*D*), brain and testis of the rat (*E*), and human brain (*F*). PCR using reverse-transcribed cDNAs from the same amount of total RNAs was performed with the predetermined optimal cycle for each primer set. RT-PCR products obtained with the same primer sets for RNAs derived from the same species were loaded and separated on the same agarose gel. The *GAPDH* gene was used as control.
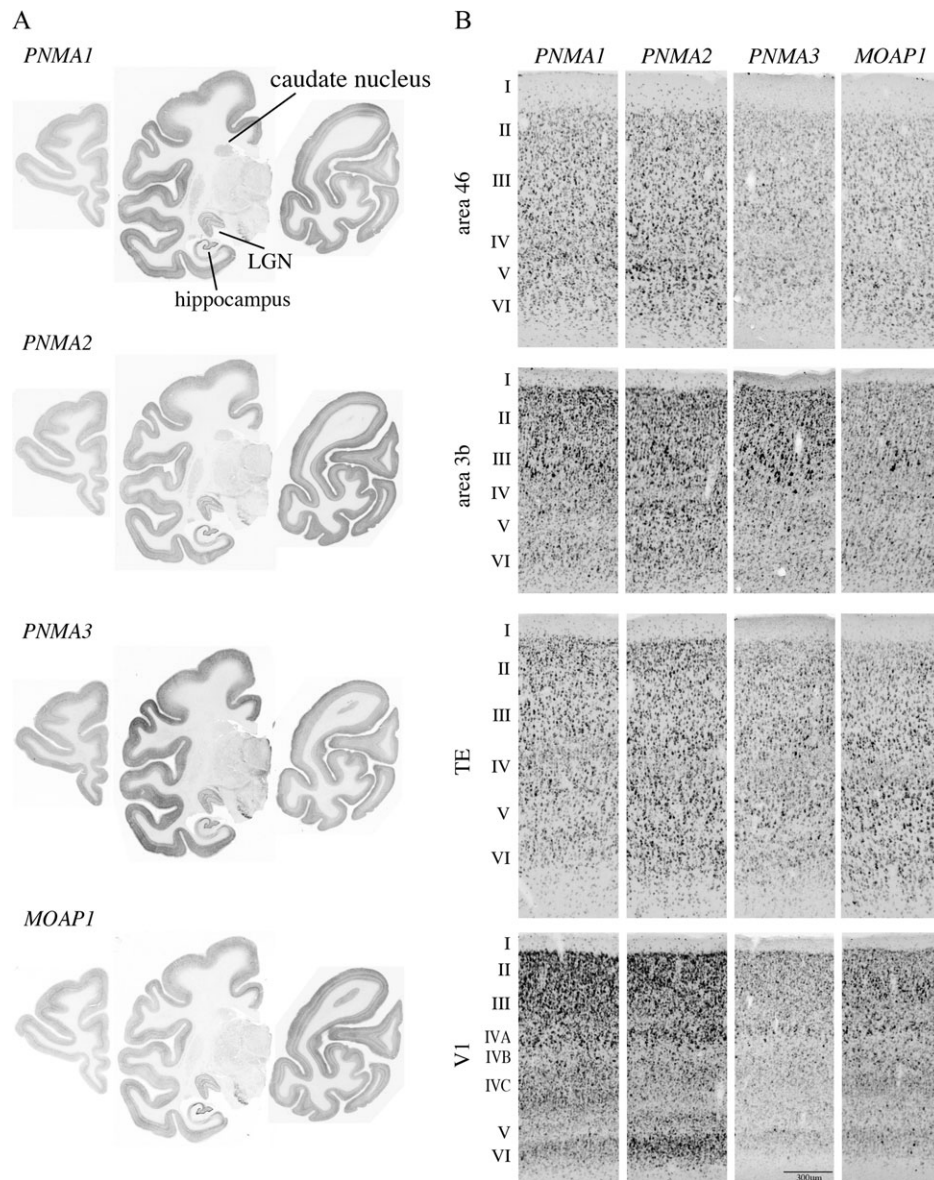
Figure 7. Expression patterns of the family genes of *PNMA5* in the macaque neocortex. (*A*) Coronal sections at positions *A*, *E*, and *G* in Figure 2 are shown. (*B*) Higher magnifications of area 46, area 3b, TE and V1. The layers indicated on the left side of each panel were identified according to the Nissl staining of the nearby section.

inferotemporal and perirhinal cortices, is widely distributed in layers Ib, II, III, V, and VI (Ichinohe and Rockland 2005; Miyashita et al. 2007). Zn is considered to be a neuromodulator associated with activity-dependent synaptic plasticity (Dyck et al. 2003). The similarity in distribution of *PNMA5* and *RBP* mRNA expressions and of synaptic Zn suggests that the expression patterns for the mRNAs of the 2 genes may represent regions of highly neuronal plasticity (Murayama et al. 1997). The expression patterns of *PNMA5* and *RBP* mRNAs are not identical (i.e., they have varying intensities at the level of single cells) but are overall very similar. This may be interpreted to mean that the expression of the 2 genes reflects extracellular environmental factors, rather than the cell autonomous properties of cortical neurons. That is, the similar expression patterns may be a signal of common responses to microcircuits and/or microenvironments, which are specifically dedicated to associative functions. Therefore, *PNMA5*

mRNA expression in monkeys may reflect increasing associative functions of the neocortex during primate evolution.

Potential Functions of PNMA *Family Genes in Mammalian Brains*

What would be the molecular functions of *RBP* and *PNMA* genes in the brain? RBP protein is suggested to have a role in maintaining higher brain function, and disruption of RBP-mediated retinoid metabolism is associated with some mental disorders and dementias, for example, Alzheimer's disease (Goodman and Pardee 2003; Puchades et al. 2003), schizophrenia (Goodman, 1998), and frontotemporal dementia (Davidsson et al. 2002). Despite similarity in the expression pattern, the amino acid sequences of *PNMA5* and its family of genes show no similarity to that of *RBP* or the other genes that are involved in the retinol metabolism.

PNMA1, PNMA2, and PNMA3 proteins were first identified as antigens in the sera of patients with paraneoplastic
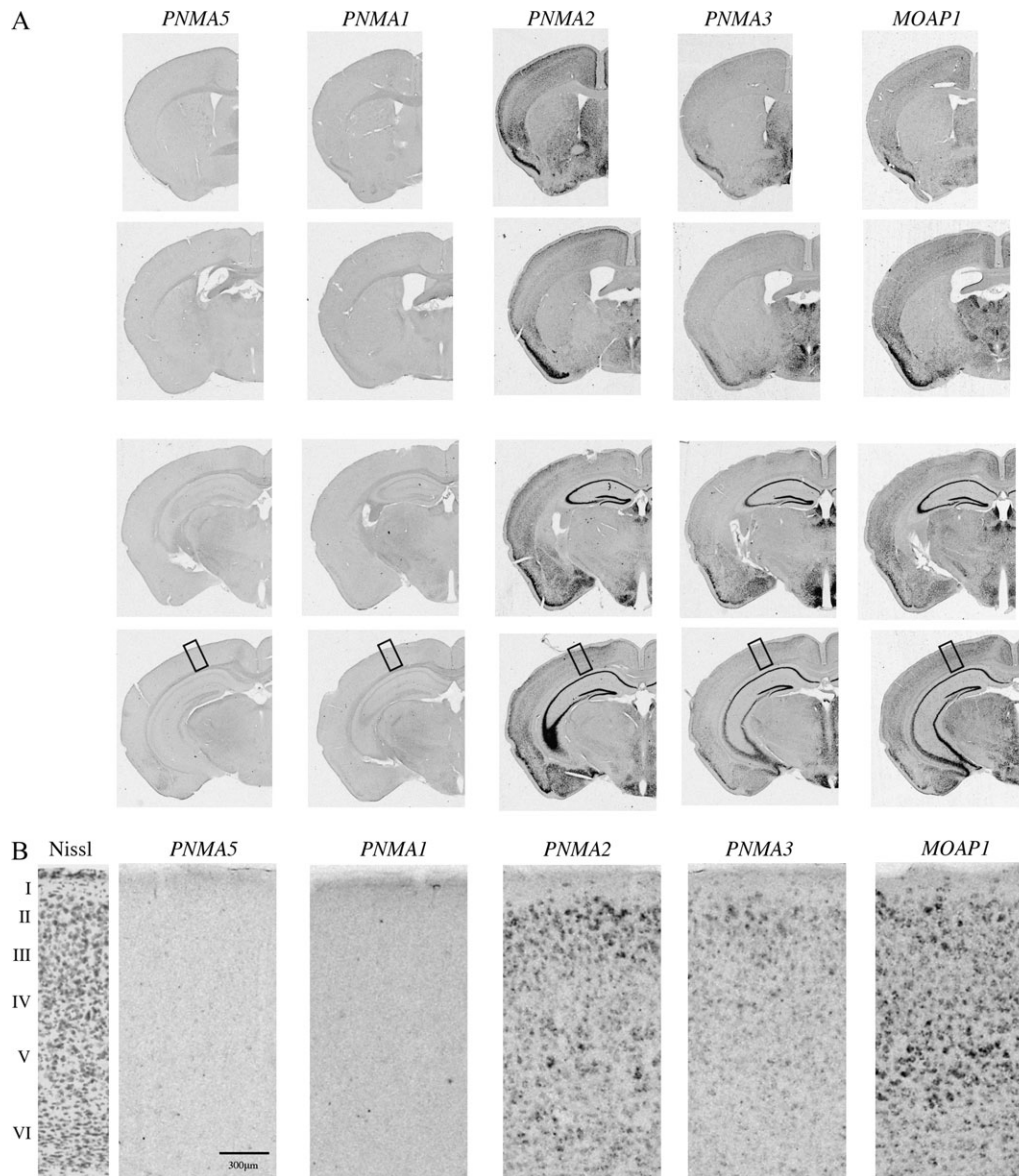
Figure 8. ISH of *PNMA5* and the *PNMA* family genes in the mouse brains. (*A*) Coronal sections at several different planes for each gene are shown. The boxed region (V1) of each gene is shown in *B* at higher magnification. (*B*) The layers indicated on the left side are identified according to the Nissl staining of the nearby section.

neurological disorders (Dalmau et al. 1999; Voltz et al. 1999; Rosenfeld et al. 2001). Immunohistochemistry using these sera showed that these 3 proteins mainly localize in the nucleoli, although some of them are in the cytoplasm. On the basis of this subcellular localization and the presence of a zinc-finger motif, PNMA3 protein was suggested to play a role in mRNA biogenesis (Dalmau et al. 1999; Voltz et al. 1999; Rosenfeld et al. 2001). MOAP1 protein (PNMA4) was identified as a binding partner of a proapoptotic Bcl-2 member, Bax, and is capable of triggering cytochrome *c*-mediated apoptosis on contact with death receptors (TNF-R1 or TRAIL-R1) and tumor suppressor RASSF1A in mammalian cells (Tan et al. 2001; Baksh et al. 2005; Tan et al. 2005; Vos et al. 2006; Foley et al. 2008). However, considering the abundant expression of *MOAP1* mRNA in the mature cortical neurons in monkeys and mice, we think that it is unlikely to induce apoptosis in normal adult brains. Consistent with this, a recent study has shown that upregulated

MOAP1 protein cannot induce apoptosis in SY5Y human neuroblastoma cells (Fu et al. 2007). In our material, overexpression of the MOAP1 protein also did not trigger apoptosis in Neuro2a mouse neuroblastoma cells (M.T. and T.Y. unpublished observation). We observed that the PNMA5 protein overexpressed in Neuro2a localize in the nucleus (M.T. and T.Y. unpublished observation). To summarize, there is good evidence for the subcellular localizations of these *PNMA* family genes (i.e., the *PNMA* family proteins are likely to be present in the cytoplasm or nucleus unlike RBP protein, which is mainly in the plasma), but the molecular functions in the brain are still largely unknown.

What is intriguing about the *PNMA* family genes is that their mRNA expression patterns differ markedly across different mammalian species. For example, although *PNMA1* mRNA is expressed widely in various monkey tissues including the brain, its expression in mice is restricted to the testis, despite the

high level of *PNMA1* gene sequence conservation (92.1% identity between human and mouse amino acid sequences). Similarly, the mouse orthologue of the *PNMA5* gene, which shows a characteristic expression pattern in monkey brains, is not detected in the mouse brain. Whereas *PNMA3* mRNA is not expressed in mouse testis, *MOAP1* mRNA expression is higher in the mouse testis than in the monkey testis. One possibility for this expression difference would be that *PNMA* family genes share common features that can compensate for each other. On the other hand, the species-specific expression also suggests that each gene in the *PNMA* family evolved specialized functions. The common functions and species-specific roles of the *PNMA* gene family in neural tissues remain to be elucidated.

Evolution of PNMA5 *Sequence and Expression along with Evolution of the Brain*

There have been long-standing debates as to whether important evolutionary changes have occurred predominantly in the gene regulatory sequences or coding sequences (King and Wilson 1975; Carroll 2003; Olson and Varki 2003). Several lines of evidence suggest that both aspects are important. For example, on the basis of human–chimpanzee comparison, King and Wilson (1975) propose that evolutionary changes in the anatomy and lifestyle are more often based on changes in the mechanisms of gene expression than on changes in the amino acid sequences. Recent microarray studies provide further evidence for large changes in the pattern of gene expression across species and suggest that such changes have played roles in evolution (Enard, Khaitovich, et al. 2002; Cáceres et al. 2003; Preuss et al. 2004; Uddin et al. 2004). On the other hand, there are also studies that support the importance of amino acid sequence changes for primate brain evolution. For example, nervous system–related genes display significantly higher rates of protein evolution in primates than in rodents (Dorus et al. 2004). Furthermore, *ASPM* and *MCPH1* genes, which are involved in regulating brain size during development (Bond et al. 2002; Jackson et al. 2002), show significantly accelerated rates of amino acid changes along the lineages leading to humans (Zhang 2003; Evans, Anderson, Vallender, Choi, et al. 2004; Evans, Anderson, Vallender, Gilbert et al. 2004; Kouprina et al. 2004; Wang and Su 2004). The *FOXP2* gene, whose mutation is associated with a speech and language disorder in humans (Lai et al. 2001), also shows significantly accelerated amino acid changes along the lineages leading to humans (Enard, Przeworski, et al. 2002; Zhang et al. 2002). These results suggest a possible link between alterations in protein sequences and the phenotypic evolution of the human brain.

In this study, we observed differences in the *PNMA* family genes in terms of both amino acid sequences and mRNA expressions between primates and rodents. Of particular interest is the divergence of the *PNMA5* sequence and expression pattern. The human and mouse amino acid sequences encoded by the *PNMA5* gene are only 57.0% identical, which is far below the average human–mouse homology (86.4%, Makalowski and Boguski 1998). This suggests that *PNMA5* has acquired a unique function during primate evolution. The characteristic area and lamina expression patterns of *PNMA5* mRNA and the sequence divergence in mammals suggest its involvement in functions particular to association areas in the neocortex of primates.

Supplementary Material

Notes

References

Abramoff MD, Magelhaes PJ, Ram SJ. 2004. Image processing with ImageJ. Biophotonics Int. 11:36–42.

Amir Y, Harel M, Malach R. 1993. Cortical hierarchy reflected in the organization of intrinsic connections in macaque monkey visual cortex. J Comp Neurol. 334:19–46.

Andersen RA. 1989. Visual and eye movement functions of the posterior parietal cortex. Annu Rev Neurosci. 12:377–403.

Baksh S, Tommasi S, Fenton S, Yu VC, Martins LM, Pfeifer GP, Latif F, Downward J, Neel BG. 2005. The tumor suppressor RASSF1A and MAP-1 link death receptor signaling to Bax conformational change and cell death. Mol Cell. 18:637–650.

Baylis GC, Rolls ET, Leonard CM. 1987. Functional subdivisions of the temporal lobe neocortex. J Neurosci. 7:330–342.

Bignall KE, Imbert M. 1969. Polysensory and cortico-cortical projections to frontal lobe of squirrel and rhesus monkeys. Electroencephalogr Clin Neurophysiol. 26:206–215.

Bloom FE, Björklund A, Hökfelt T. 1997. The primate nervous system. In Handbook of chemical neuroanatomy. Amsterdam, New York: Elsevier.

Bond J, Roberts E, Mochida GH, Hampshire DJ, Scott S, Askham JM, Springell K, Mahadevan M, Crow YJ, Markham AF, et al. 2002. ASPM is a major determinant of cerebral cortical size. Nat Genet. 32:316–320.

Brodmann K. 1909. Vergleichende Lokalisationlehre der Grosshirnrinde in ihren Prinzipien dargestellt auf Grund des Zellenbaues. Leipzig (Germany): Barth (Reprinted as Brodmann's "Localisation in the cerebral cortex," translated and edited by Garey LJ, London: Smith-Gordon, 1994).

Brodmann K. 1912. Neue Ergibnisse uber die vergleichende histologische Lokalisation der Grosshirnrinde mit besonderer Berucksichtigung des Stirnhirns. Anat Anz. 41(Suppl):157–216.

Bruce C, Desimone R, Gross CG. 1981. Visual properties of neurons in a polysensory area in superior temporal sulcus of the macaque. J Neurophysiol. 46:369–384.

Cáceres M, Lachuer J, Zapala MA, Redmond JC, Kudo L, Geschwind DH, Lockhart DJ, Preuss TM, Barlow C. 2003. Elevated gene expression levels distinguish human from non-human primate brains. Proc Natl Acad Sci USA. 100:13030-13035.

Carroll SB. 2003. Genetics and the making of *Homo sapiens*. Nature. 422:849–857.

Chomczynski P, Sacchi N. 1987. Single-step method of RNA isolation by acid guanidinium thiocyanate–phenol–chloroform extraction. Anal Biochem. 162:156–159.

Crick F. 1999. The impact of molecular biology on neuroscience. Philos Trans R Soc Lond B Biol Sci. 354:2021–2025.

Dalmau J, Gultekin SH, Voltz R, Hoard R, DesChamps T, Balmaceda C, Batchelor T, Gerstner E, Eichen J, Frennier J, et al. 1999. Ma1, a novel neuron- and testis-specific protein, is recognized by the serum of patients with paraneoplastic neurological disorders. Brain. 122:27–39.

Davidsson P, Sjögren M, Andreasen N, Lindbjer M, Nilsson CL, Westman-Brinkmalm A, Blennow K. 2002. Studies of the pathophysiological mechanisms in frontotemporal dementia by proteome analysis of CSF proteins. Brain Res Mol Brain Res. 109:128–133.

Dorus S, Vallender EJ, Evans PD, Anderson JR, Gilbert SL, Mahowald M, Wyckoff GJ, Malcom CM, Lahn BT. 2004. Accelerated evolution of nervous system genes in the origin of Homo sapiens. Cell. 119:1027–1040.

Dyck RH, Chaudhuri A, Cynader MS. 2003. Experience-dependent regulation of the zincergic innervation of visual cortex in adult monkeys. Cereb Cortex. 13:1094–1109.

Elston GN. 2000. Pyramidal cells of the frontal lobe: all the more spinous to think with. J Neurosci. 20:RC95.

Elston GN, Tweedale R, Rosa MG. 1999. Cortical integration in the visual system of the macaque monkey: large-scale morphological differences in the pyramidal neurons in the occipital, parietal and temporal lobes. Proc Biol Sci. 266:1367–1374.

Enard W, Khaitovich P, Klose J, Zöllner S, Heissig F, Giavalisco P, Nieselt-Struwe K, Muchmore E, Varki A, Ravid R, et al. 2002. Intra- and interspecific variation in primate gene expression patterns. Science. 296:340–343.

Enard W, Przeworski M, Fisher SE, Lai CS, Wiebe V, Kitano T, Monaco AP, Pääbo S. 2002. Molecular evolution of FOXP2, a gene involved in speech and language. Nature. 418:869–872.

Evans PD, Anderson JR, Vallender EJ, Choi SS, Lahn BT. 2004. Reconstructing the evolutionary history of microcephalin, a gene controlling human brain size. Hum Mol Genet. 13:1139–1145.

Evans PD, Anderson JR, Vallender EJ, Gilbert SL, Malcom CM, Dorus S, Lahn BT. 2004. Adaptive evolution of ASPM, a major determinant of cerebral cortical size in humans. Hum Mol Genet. 13:489–494.

Evans SJ, Choudary PV, Vawter MP, Li J, Meador-Woodruff JH, Lopez JF, Burke SM, Thompson RC, Myers RM, et al. 2003. DNA microarray analysis of functionally discrete human brain regions reveals divergent transcriptional profiles. Neurobiol Dis. 14:240–250.

Finlay BL, Darlington RB. 1995. Linked regularities in the development and evolution of mammalian brains. Science. 268:1578–1584.

Foley CJ, Freedman H, Choo SL, Onyskiw C, Fu NY, Yu VC, Tuszynski J, Pratt JC, Baksh S. 2008. Dynamics of RASSF1A/MOAP-1 association with death receptors. Mol Cell Biol. 28:4520–4535.

Freese JL, Amaral DG. 2005. The organization of projections from the amygdala to visual cortical areas TE and V1 in the macaque monkey. J Comp Neurol. 486:295–317.

Friedman DP, Murray EA, O'Neill JB, Mishkin M. 1986. Cortical connections of the somatosensory fields of the lateral sulcus of macaques: evidence for a corticolimbic pathway for touch. J Comp Neurol. 252:323–347.

Fu NY, Sukumaran SK, Yu VC. 2007. Inhibition of ubiquitin-mediated degradation of MOAP-1 by apoptotic stimuli promotes Bax function in mitochondria. Proc Natl Acad Sci USA. 104:10051–10056.

Galaburda AM, Pandya DN. 1983. The intrinsic architectonic and connectional organization of the superior temporal region of the rhesus monkey. J Comp Neurol. 221:169–184.

Goldman-Rakic PS. 1988. Topography of cognition: parallel distributed networks in primate association cortex. Annu Rev Neurosci. 11:137–156.

Goodman AB. 1998. Three independent lines of evidence suggest retinoids as causal to schizophrenia. Proc Natl Acad Sci USA. 95:7240–7244.

Goodman AB, Pardee AB. 2003. Evidence for defective retinoid transport and function in late onset Alzheimer's disease. Proc Natl Acad Sci USA. 100:2901–2905.

Gur M, Snodderly DM. 2008. Physiological differences between neurons in layer 2 and layer 3 of primary visual cortex (V1) of alert macaque monkeys. J Physiol. 586:2293–2306.

Haug H. 1987. Brain sizes, surfaces, and neuronal sizes of the cortex cerebri: a stereological investigation of man and his variability and a comparison with some mammals (primates, whales, marsupials, insectivores, and one elephant). Am J Anat. 180:126–142.

Ichinohe N, Rockland KS. 2005. Zinc-enriched amygdalo- and hippo-campo-cortical connections to the inferotemporal cortices in macaque monkey. Neurosci Res. 53:57–68.

Jackson AP, Eastwood H, Bell SM, Adu J, Toomes C, Carr IM, Roberts E, Hampshire DJ, Crow YJ, Mighell AJ, et al. 2002. Identification of microcephalin, a protein implicated in determining the size of the human brain. Am J Hum Genet. 71:136–142.

Jones EG, Powell TP. 1970. An anatomical study of converging sensory pathways within the cerebral cortex of the monkey. Brain. 93:793–820.

Kennedy H, Bullier J. 1985. A double-labeling investigation of the afferent connectivity to cortical areas V1 and V2 of the macaque monkey. J Neurosci. 5:2815–2830.

King MC, Wilson AC. 1975. Evolution at two levels in humans and chimpanzees. Science. 188:107–116.

Komatsu Y, Watakabe A, Hashikawa T, Tochitani S, Yamamori T. 2005. Retinol-binding protein gene is highly expressed in higher-order association areas of the primate neocortex. Cereb Cortex. 15:96–108.

Kouprina N, Pavlicek A, Mochida GH, Solomon G, Gersch W, Yoon YH, Collura R, Ruvolo M, Barrett JC, Woods CG, et al. 2004. Accelerated evolution of the ASPM gene controlling brain size begins prior to human brain expansion. PLoS Biol. 2:E126.

Lai CS, Fisher SE, Hurst JA, Vargha-Khadem F, Monaco AP. 2001. A forkhead-domain gene is mutated in a severe speech and language disorder. Nature. 413:519–523.

Leinonen L, Hyvärinen J, Sovijärvi AR. 1980. Functional properties of neurons in the temporo-parietal association cortex of awake monkey. Exp Brain Res. 39:203–215.

Liang F, Hatanaka Y, Saito H, Yamamori T, Hashikawa T. 2000. Differential expression of gamma-aminobutyric acid type B receptor-1a and -1b mRNA variants in GABA and non-GABAergic neurons of the rat brain. J Comp Neurol. 416:475–495.

Lund JS, Yoshioka T, Levitt JB. 1993. Comparison of intrinsic connectivity in different areas of macaque monkey cerebral cortex. Cereb Cortex. 3:148–162.

Makalowski W, Boguski MS. 1998. Evolutionary parameters of the transcribed mammalian genome: an analysis of 2,820 orthologous rodent and human sequences. Proc Natl Acad Sci USA. 95:9407–9412.

Mash DC, White WF, Mesulam MM. 1988. Distribution of muscarinic receptor subtypes within architectonic subregions of the primate cerebral cortex. J Comp Neurol. 278:265–274.

Mesulam MM, Van Hoesen GW, Pandya DN, Geschwind N. 1977. Limbic and sensory connections of the inferior parietal lobule (area PG) in the rhesus monkey: a study with a new method for horseradish peroxidase histochemistry. Brain Res. 136:393–414.

Milner B, Petrides M. 1984. Behavioural effects of frontal-lobe lesions in man. Trends Neurosci. 7:403–407.

Miyashita T, Ichinohe N, Rockland KS. 2007. Differential modes of termination of amygdalothalamic and amygdalocortical projections in the monkey. J Comp Neurol. 502:309–324.

Murayama Y, Fujita I, Kato M. 1997. Contrasting forms of synaptic plasticity in monkey inferotemporal and primary visual cortices. Neuroreport. 8:1503–1508.

Nealey TA, Maunsell JH. 1994. Magnocellular and parvocellular contributions to the responses of neurons in macaque striate cortex. J Neurosci. 14:2069–2079.

Olson MV, Varki A. 2003. Sequencing the chimpanzee genome: insights into human evolution and disease. Nat Rev Genet. 4:20–28.

Pandya DN, Kuypers HG. 1969. Cortico-cortical connections in the rhesus monkey. Brain Res. 13:13–36.

Pandya DN, Seltzer B. 1982. Association areas of the cerebral cortex. Trends Neurosci. 5:386–390.

Pandya DN, Yeterian EH. 1990. Prefrontal cortex in relation to other cortical areas in rhesus monkey: architecture and connections. Prog Brain Res. 85:63–94.

Paxinos G, Huang X-F, Toga AW. 1999. The rhesus monkey brain in stereotaxic coordinates. San Diego (CA): Academic Press.

Pfeffer BA, Becerra SP, Borst DE, Wong P. 2004. Expression of transthyretin and retinol binding protein mRNAs and secretion of transthyretin by cultured monkey retinal pigment epithelium. Mol Vis. 10:23–30.

Pimenta AF, Strick PL, Levitt P. 2001. Novel proteoglycan epitope expressed in functionally discrete patterns in primate cortical and subcortical regions. J Comp Neurol. 430:369–388.

Preuss TM, Cáceres M, Oldham MC, Geschwind DH. 2004. Human brain evolution: insights from microarrays. Nat Rev Genet. 5:850–860.

Preuss TM, Goldman-Rakic PS. 1991a. Myelo- and cytoarchitecture of the granular frontal cortex and surrounding regions in the strepsirhine primate Galago and the anthropoid primate Macaca. J Comp Neurol. 310:429–474.

Preuss TM, Goldman-Rakic PS. 1991b. Architectonics of the parietal and temporal association cortex in the strepsirhine primate Galago compared to the anthropoid primate Macaca. J Comp Neurol. 310:475–506.

Preuss TM, Goldman-Rakic PS. 1991c. Ipsilateral cortical connections of granular frontal cortex in the strepsirhine primate Galago, with comparative comments on anthropoid primates. J Comp Neurol. 310:507–549.

Puchades M, Hansson SF, Nilsson CL, Andreasen N, Blennow K, Davidsson P. 2003. Proteomic studies of potential cerebrospinal fluid protein markers for Alzheimer's disease. Brain Res Mol Brain Res. 118:140–146.

Rockland KS, Saleem KS, Tanaka K. 1994. Divergent feedback connections from areas V4 and TEO in the macaque. Vis Neurosci. 11:579–600.

Rockland KS, Virga A. 1989. Terminal arbors of individual "feedback" axons projecting from area V2 to V1 in the macaque monkey: a study using immunohistochemistry of anterogradely transported Phaseolus vulgaris-leucoagglutinin. J Comp Neurol. 285:54–72.

Rosenfeld MR, Eichen JG, Wade DF, Posner JB, Dalmau J. 2001. Molecular and clinical diversity in paraneoplastic immunity to Ma proteins. Ann Neurol. 50:339–348.

Sambrook J, Fritsch T, Maniatis T. 1989. Molecular cloning—a laboratory manual. Cold Spring Harbor (NY): Cold Spring Harbor Laboratory Press.

Sato A, Nishimura Y, Oishi T, Higo N, Murata Y, Onoe H, Saito K, Tsuboi F, Takahashi M, Isa T, et al. 2007. Differentially expressed genes among motor and prefrontal areas of macaque neocortex. Biochem Biophys Res Commun. 362:665–669.

Schüller M, Jenne D, Voltz R. 2005. The human PNMA family: novel neuronal proteins implicated in paraneoplastic neurological disease. J Neuroimmunol. 169:172–176.

Shintani T, Kato A, Yuasa-Kawada J, Sakuta H, Takahashi M, Suzuki R, Ohkawara T, Takahashi H, Noda M. 2004. Large-scale identification and characterization of genes with asymmetric expression patterns in the developing chick retina. J Neurobiol. 59:34–47.

Shipp S, Zeki S. 2002. The functional organization of area V2, I: specialization across stripes and layers. Vis Neurosci. 19:187–210.

Stephan H, Frahm H, Baron G. 1981. New and revised data on volumes of brain structures in insectivores and primates. Folia Primatol (Basel). 35:1–29.

Suzuki H, Yaoi T, Kawai J, Hara A, Kuwajima G, Watanabe S. 1996. Restriction landmark cDNA scanning (RLCS): a novel cDNA display system using two-dimensional gel electrophoresis. Nucleic Acids Res. 24:289–294.

Takahata T, Komatsu Y, Watakabe A, Hashikawa T, Tochitani S, Yamamori T. 2006. Activity-dependent expression of occ1 in excitatory neurons is a characteristic feature of the primate visual cortex. Cereb Cortex. 16:929–940.

Takahata T, Komatsu Y, Watakabe A, Hashikawa T, Tochitani S, Yamamori T. 2008. Differential expression patterns of occ1-related genes in adult monkey visual cortex. Cereb Cortex. Epub ahead of print.

Takamori S, Rhee JS, Rosenmund C, Jahn R. 2000. Identification of a vesicular glutamate transporter that defines a glutamatergic phenotype in neurons. Nature. 407:189–194.

Tan KO, Fu NY, Sukumaran SK, Chan SL, Kang JH, Poon KL, Chen BS, Yu VC. 2005. MAP-1 is a mitochondrial effector of Bax. Proc Natl Acad Sci USA. 102:14623–14628.

Tan KO, Tan KM, Chan SL, Yee KS, Bevort M, Ang KC, Yu VC. 2001. MAP-1, a novel proapoptotic protein containing a BH3-like motif that associates with Bax through its Bcl-2 homology domains. J Biol Chem. 276:2802–2807.

Tanigawa H, Wang Q, Fujita I. 2005. Organization of horizontal axons in the inferior temporal cortex and primary visual cortex of the macaque monkey. Cereb Cortex. 15:1887–1899.

Tigges J, Spatz WB, Tigges M. 1973. Reciprocal point-to-point connections between parastriate and striate cortex in the squirrel monkey (Saimiri). J Comp Neurol. 148:481–489.

Tochitani S, Liang F, Watakabe A, Hashikawa T, Yamamori T. 2001. The occ1 gene is preferentially expressed in the primary visual cortex in an activity-dependent manner: a pattern of gene expression related to the cytoarchitectonic area in adult macaque neocortex. Eur J Neurosci. 13:297–307.

Uddin M, Wildman DE, Liu G, Xu W, Johnson RM, Hof PR, Kapatos G, Grossman LI, Goodman M. 2004. Sister grouping of chimpanzees and humans as revealed by genome-wide phylogenetic analysis of brain gene expression profiles. Proc Natl Acad Sci USA. 101: 2957–2962.

Ullman S. 1995. Sequence seeking and counter streams: a computational model for bidirectional information flow in the visual cortex. Cereb Cortex. 5:1–11.

Van Hoesen GW. 1982. The parahippocampal gyrus: new observations regarding its cortical connections in the monkey. Trends Neurosci. 5:345–350.

Voltz R, Gultekin SH, Rosenfeld MR, Gerstner E, Eichen J, Posner JB, Dalmau J. 1999. A serologic marker of paraneoplastic limbic and brain-stem encephalitis in patients with testicular cancer. N Engl J Med. 340:1788–1795.

Vos MD, Dallol A, Eckfeld K, Allen NP, Donninger H, Hesson LB, Calvisi D, Latif F, Clark GJ. 2006. The RASSF1A tumor suppressor activates Bax via MOAP-1. J Biol Chem. 281:4557–4563.

Wang YQ, Su B. 2004. Molecular evolution of microcephalin, a gene determining human brain size. Hum Mol Genet. 13:1131–1137.

Watakabe A, Fujita H, Hayashi M, Yamamori T. 2001. Growth/differentiation factor 7 is preferentially expressed in the primary motor area of the monkey neocortex. J Neurochem. 76:1455–1464.

Watakabe A, Ichinohe N, Ohsawa S, Hashikawa T, Komatsu Y, Rockland KS, Yamamori T. 2007. Comparative analysis of layer-specific genes in mammalian neocortex. Cereb Cortex. 17:1918–1933.

Watakabe A, Komatsu Y, Nawa H, Yamamori T. 2006. Gene expression profiling of primate neocortex: molecular neuroanatomy of cortical areas. Genes Brain Behav. 5(Suppl 1):38–43.

Watakabe A, Komatsu Y, Sadakane O, Shimegi S, Takahata T, Higo N, Tochitani S, Hashikawa T, Naito T, Osaki H, et al. 2008. Enriched expression of serotonin 1B and 2A receptor genes in macaque visual cortex and their bidirectional modulatory effects on neuronal responses. Cereb Cortex. Epub ahead of print.

Watakabe A, Sugai T, Nakaya N, Wakabayashi K, Takahashi H, Yamamori T, Nawa H. 2001. Similarity and variation in gene expression among human cerebral cortical subregions revealed by DNA macroarrays: technical consideration of RNA expression profiling from postmortem samples. Brain Res Mol Brain Res. 88: 74–82.

Yamamori T, Rockland KS. 2006. Neocortical areas, layers, connections, and gene expression. Neurosci Res. 55:11–27.

Zhang J. 2003. Evolution of the human ASPM gene, a major determinant of brain size. Genetics. 165:2063–2070.

Zhang J, Webb DM, Podlaha O. 2002. Accelerated protein evolution and origins of human-specific features: Foxp2 as an example. Genetics. 162:1825–1835.

Zilles K, Palomero-Gallagher N, Grefkes C, Scheperjans F, Boy C, Amunts K, Schleicher A. 2002. Architectonics of the human cerebral cortex and transmitter receptor fingerprints: reconciling functional neuroanatomy and neurochemistry. Eur Neuropsychopharmacol. 12:587–599.